Nuclear Engineering and Technology 51 (2019) 269–274

Contents lists available at ScienceDirect

Nuclear Engineering and Technology

journal homepage: www.elsevier.com/locate/net

Original Article

Modeling and experimental production yield of ^{64}Cu with ^{nat}Cu and ^{nat}Cu-NPs in Tehran Research Reactor

Zahra Karimi [a], Mahdi Sadeghi [b, *], Arsalan Ezati [c]

[a] Department of Medical Radiation Engineering, Science and Research Branch, Islamic Azad University, Tehran, Iran
[b] Medical Physics Department, School of Medicine, Iran University of Medical Science, P.O. Box, 14155-6183, Tehran, Iran
[c] Nuclear Science & Technology Research Institute (NSTRI), Reactor and Nuclear Safety Research School, P.O. Box, 14395-836, Tehran, Iran

ARTICLE INFO

Article history:
Received 15 July 2018
Received in revised form
11 August 2018
Accepted 12 August 2018
Available online 13 August 2018

Keywords:
^{64}Cu radioisotope
Copper nanoparticles
Production yield
MCNPX
TALYS-1.8

ABSTRACT

^{64}Cu is a favorable radionuclide in nuclear medicine applications because of its unique characteristics such as three types of decay (electron capture, β^- and β^+) and 12.7 h half-life. Production of ^{64}Cu by irradiation ^{nat}Cu and ^{nat}CuNPs in Tehran Research Reactor was investigated. The characteristics of copper nanoparticles were investigated with SEM, TEM and XRD analysis. The cross section of ^{63}Cu(n,γ)^{64}Cu reaction was done with TALYS-1.8 code. The activity value of ^{64}Cu was calculated with theoretical approach and MCNPX-2.6 code. The results were compared with related experimental results which showed good adaptations between them.

1. Introduction

The ^{64}Cu is a unique radionuclide ($T_{1/2}$ = 12.7 h) with decay mode of E.C. (43.53%), β^- (38.48%) and β^+ (17.52%); End-point E_{β}^{+} = 653 keV, End-point E_{β}^{-} = 579 keV, Eγ = 1345.84 keV, I_{γ} = 0.47% (Fig. 1). According to these properties, ^{64}Cu is described as a useful radionuclide for both high resolution Positron Emission Tomography (PET) imaging and targeted endoradiotherapy. When this radionuclide is deposited in the cell, its electron capture decay can be more efficient in cell killing [1].

^{64}Cu can be produced with ^{nat}Cu(n,γ)^{64}Cu and ^{63}Cu(n,γ)^{64}Cu reactions in nuclear reactor [3–5]. The advantages of this reaction are abundant thermal neutrons and large cross sections. In 2010, the cross section of this reaction was reported by Cohen and et al. about 4.5 ± 0.1 b via thermal neutron induce reaction respectively [5]. These values are reasonably high for medical applications in comparison with some other radionuclides which can be produced with thermal neutron such as ^{123}Sn (σ_{th} = 0.183 b), ^{103}Ru (σ_{th} = 1.23 b), ^{113}Sn (σ_{th} = 1.14 b), ^{141}Ce (σ_{th} = 0.575 b) and ^{197}Pt (σ_{th} = 0.74 b) [6]. The Disadvantages are no simple chemical separation and low specific activity [7], while use of fast neutrons are compulsory for high specific activity of ^{64}Cu via ^{64}Zn(n,p)^{64}Cu reaction [3].

The Application of nanoparticles on ^{64}Cu production has its objective. The most important characteristic of radioactive nanoparticles is its ability to have several radioactive atoms in one single nanoparticle [8]. In our previous work, we researched on ^{64}Cu production with ^{nat}ZnO and ^{nat}ZnONPs targets via ^{nat}Zn(n,p)^{64}Cu reaction. We concluded that the activity of ^{64}Cu with nano scale target was increased [9]. Other researches in this subject were ^{198}Au, ^{141}Ce, ^{142}Pr radionuclides productions [8,10–12].

In this research ^{64}Cu was produced with 1 g of ^{nat}CuNPs and ^{nat}Cu powders with natural abundance via the ^{63}Cu(n,γ)^{64}Cu reaction in Tehran Research Reactor (TRR). The activity of ^{64}Cu from bulk and nano scale targets at the End of Bombardment (EOB) was compared with each other. The Transmission Electronic Microscopy (TEM), Scanning Electronic Microscopy (SEM) and X-Ray Diffraction (XRD) analysis for determining ^{nat}CuNPs characteristics before and after irradiation were done. The theoretical activity of ^{64}Cu was calculated by using the MCNPX and TALYS codes and was compared with corresponding experimental value.

* Corresponding author.
E-mail address: sadeghi.m@iums.ac.ir (M. Sadeghi).

https://doi.org/10.1016/j.net.2018.08.008

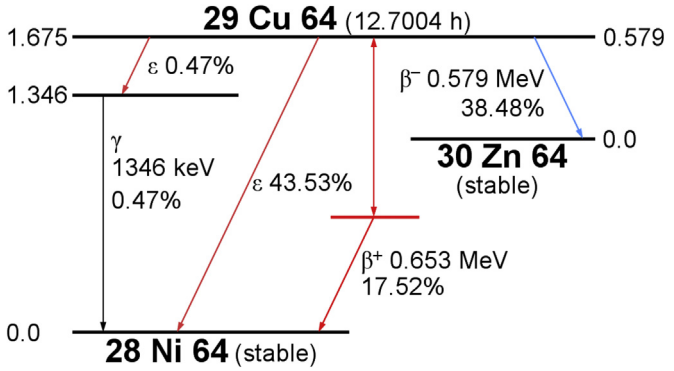

Fig. 1. The decay scheme of the ^{64}Cu radionuclide [2].

2. Material and methods

2.1. Material

The natural copper has two stable isotopes which are ^{63}Cu with abundance of 69.17% and ^{65}Cu with abundance of 30.83%. All chemical powders were purchased from US Research Nanomaterials, Inc. (Houston, USA). Physical properties and chemical composition of powders are presented in Table 1.

2.2. Theoretical activity calculation

The activity of the product can be calculated with the following equation [13]:

$$A = N.\sigma.\Phi.\left(1 - e^{-\lambda t_{irr}}\right).D_C \quad (1)$$

Where A is the activity in Bq after an irradiation period of t_{irr}, $N = \frac{m.H_i.N_A}{M}$ is the number of target's atom with the weight of target (m), abundance of ^{63}Cu (H_i), Avogadro's Number (N_A) and molar mass of target (M), σ is the thermal neutron capture cross section, Φ is the thermal neutron flux, λ is the decay constant of ^{64}Cu and $D_c = e^{-\lambda T}$ is a constant for determining the activity after cool down period (T). The activity of target under irradiation process is increased with exponential factor in Eq. (1) and reaches maximum saturation value, but the activity of target after irradiation time is decreased with exponential factor in the D_c constant.

2.3. Cross section calculation

In this investigation, cross sections of ^{63}Cu(n,γ)^{64}Cu reaction was calculated with TALYS-1.8 nuclear code. The results were compared with ENDF/B-VII.1 and experimental data which are available in EXFOR library. The ENDF/B-VII.1 library is theoretical nuclear data for using in nuclear science and technology applications [14]. TALYS-1.8 is the latest update version which is efficient to calculate nuclear reaction cross section [15–19]. Neutrons, photons, protons, deuterons, tritons, ^{3}He, and α-particles can be used as a projectile on target nuclei in this code with selective energy range of 1 keV–200 MeV. Several options are included such as γ-ray strength functions, nuclear level densities, nuclear model parameters and etc. while resonance parameter were used in the above-mentioned reaction as recent parameters in the latest version of TALYS code [20–24].

2.4. Description of irradiation process

The ^{64}Cu was produced with 1 g of ^{nat}Cu and ^{nat}CuNPs powders respectively. The powders were taken in quartz ampules and then flame sealed separately and was placed inside the aluminum cans for irradiating in the core of TRR. The power of reactor in this study was 4 MW with approximately thermal neutron flux of 4.5×10^{13} n.cm^{-2}.s^{-1} in the samples placement. The irradiation time for targets was 32 min and after 2 days cooling time two targets were dissolved in 20 ml 10 M HNO_3 and were diluted. The chemical processing of the irradiated targets were carried out as making homogenous solution and reasonable activity for gamma spectrometry. The production yield was estimated with a high purity p-type detector (HPGe) coupled with a multichannel analyzer (MCA) (Silena International, Rome, Italy) with a relative efficiency of 37% which calibrated with a point-like source of ^{152}Eu manufactured by Amersham Company.

2.5. Copper nanoparticles characteristics

The characteristics of copper nanoparticles were done with XRD from US Research Nanomaterials, Inc. (Houston, USA) when the nanoscale sample was not placed in the vicinity of the air. The chemical composition of ^{nat}CuNPs with XRD from (STOE STADI, MP, Germany) were done after 6 months when it was placed in the vicinity of the air. The XRD analysis is used for the crystallite size and structure of samples. The crystallite size was calculated with the Scherrer's equation (2) at a scanning rate from 5 to 90 [25].

$$Crystallite\ size\ (average) = \frac{0.89\,\lambda}{B\cos\theta} \quad (2)$$

Where 0.89 is Scherrer's constant for sphere particles, λ is the wavelength of X-Rays, θ is the Bragg diffraction angle, and β is the full width at half-maximum (FWHM) of the diffraction peak corresponding to plane. Morphology of the samples were investigated by using TEM and SEM analysis from Iranian Nanomaterials Pioneers Company, NANOSANY (Mashhad, Iran). After irradiation process, SEM images of copper nanoparticles were performed with Digital SEM, EM 3200 KYKY.

Table 1
Physical properties and chemical composition of ^{nat}CuNPs.

Physical properties								
Purity (%)	Average particle size (nm)		Specific surface area ($m^2\ g^{-1}$)		True density ($g\ cm^{-3}$)		Morphology	color
99.5	20		30–45		8.9		spherical	Saddle brown
Chemical composition (%)								
Cu	As	Sb	Pb	Sn	Fe	Ni	Bi	O
≥99.5	≤0.002	≤0.002	≤0.001	≤0.009	≤0.006	≤0.102	≤0.002	1.36

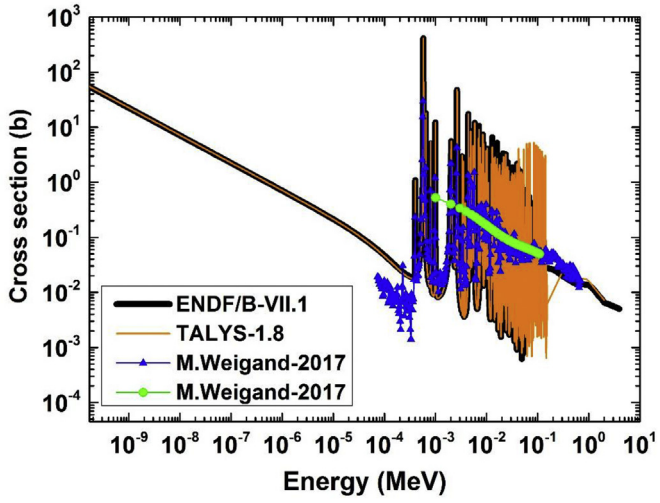

Fig. 2. Cross section of $^{63}Cu(n,\gamma)^{64}Cu$ reaction calculated by TALYS-1.8 codes along with experimental and theoretical values.

2.6. Simulation method based on MCNPX code

The MCNPX code was selected to simulate the core of TRR and defining the production yield of radionuclides. The TRR is a maximum power of 5 MW (in this work 4 MW), pool type with 9 × 6 grid plate for insertion 28 sets of fuel plates, 4 control rods, a shim safety rod, 14 packages of graphite box and 7 irradiation boxes. The fuel plates contain low enriched uranium fuel plates in the form of U_3O_8Al alloy. The reactor pool contains two sections, one of them is narrow stall end and other section is open end. The narrow stall end contains experimental facilities like beam tubes, rabbit system and thermal column. The open end section was designed for bulk irradiation [26–28].

In this methods, to calculate the ^{64}Cu production yield, The natural copper powder inside quartz ampoule and aluminum can located at the irradiation box of reactor core were described in our previous work [9,10]. The thermal neutron energy distribution $\varphi(E)$ at the ^{nat}Cu target with F4/E4 cards-MCNPX was calculated and by the results of TALYS-1.8 code the below integration were solved via the Simpson numerical integral method:

$$\varphi\sigma \approx \int_{\text{Thermal enegy region}} \varphi(E)\sigma(E)dE \qquad (3)$$

By using Eq. (1) and the result of Eq. (3), the activity of ^{64}Cu can be calculated and the value was compared with the corresponding experimental value as a benchmark data. In another way, by using the FM4 card the product saturated activity in various energy ranges were calculated.

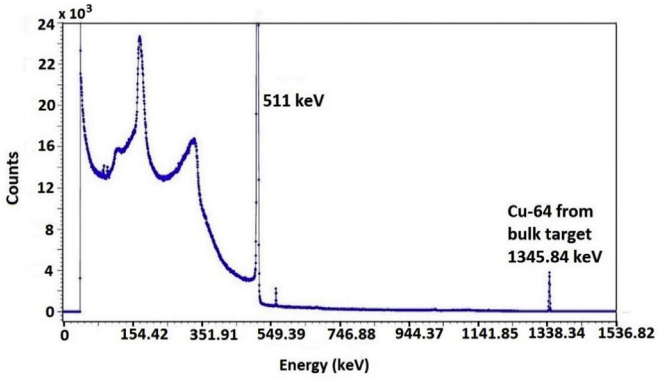

Fig. 3. Gamma spectra of ^{nat}Cu by the gamma HPGe-MCA system.

3. Results and discussion

3.1. Cross section of $^{63}Cu(n,\gamma)^{64}Cu$ reaction and theoretical activity value

Fig. 2 shows The cross section of $^{63}Cu(n,\gamma)^{64}Cu$ reaction was determined with TALYS-1.8 code and compared with the ENDF/B-VII.1 data [14] and the available experimental data [29]. There are closely connected between them in all energy regions. The calculations by the TALYS code were performed with the resonance parameter. As shown in Fig. 2 at the energy of 0.025 eV the cross section value is 4.47 b. As can be seen in Table 2, the theoretical activity value was calculated about 37.75 GBq by Eq (1) corresponding to the experimental conditions of radiation with cross section of 4.47 b.

3.2. Experimental results

Production yield of ^{64}Cu was estimated by its characteristic 1345.84 keV photopeak. The 511 keV photo peak is related to annihilation of ^{64}Cu. Figs. 3 and 4 show the spectrums of radioactive products of copper and its nanoscale targets after 80 h cooling time. The counting of gamma emission in 1345.84 keV by HPGe reached to 256 and 85 CPS after 93 min and 18 min for bulk and nanoscale targets respectively. As can be seen in Table 2, the activity value of ^{64}Cu at EOB was achieved 37.65 GBq and similarly for its nanoscale target was achieved 42.60 GBq which observed increment activity. The relative difference between two values were calculated 0.116. The ultrahigh surface-to-volume atoms ratio in the nanoscale target were increased and the properties related to the size of copper nanoparticles like cross sections and productions yield can be changed in collision with thermal neutron in nuclear reactor. The specific activity of ^{64}Cu can be increased via the long irradiation time and enriched target in less weight. ^{64}Cu is also produced via $^{65}Cu(n,2n)^{64}Cu$ reaction with cross section of 280 μb

Table 2
The activity value of ^{64}Cu at EOB with thermal neutron flux of 4.5×10^{13} n.cm^{-1}.s^{-1}.

Irradiation time (min)	Theoretical activity (GBq)		MCNPX activity (GBq)		MCNPX activity (GBq)		Experimental activity (GBq)		
	Cross section of 4.47 b	Relative Difference (with Exp. 1)	FM4-Card (GBq)	Relative Difference (with Exp. 1)	TALYS Code	Relative Difference (with Exp. 1)	Exp. 1 ^{nat}Cu target	Exp. 2 $^{nat}CuNPs$ target	Relative Difference (with Exp. 1)
32	37.75	0.003	38.15	0.013	38.32	0.017	37.65	42.60	0.116

Relative Difference: (Cal.-Exp.)/Cal.

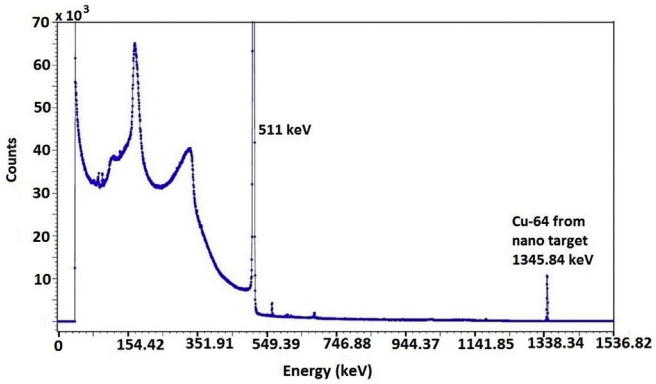

Fig. 4. Gamma spectra of ^{nat}CuNPs by the gamma HPGe-MCA system.

which was reported by Cohen and et al. [5], however the contribution in total activity is insignificant. ^{66}Cu radionuclide ($T_{1/2}$ = 5.12 m) was produced with $^{65}Cu(n,\gamma)^{66}Cu$ reaction with its characteristic 833 keV (0.22%), 1039.2 keV (9.23%) and 1332.5 keV (0.0037%) photo peaks [30] but with long period cooling time was decayed and there was not in the both spectrums of radioactive samples.

3.3. Simulation results

The neutron energy spectrum is separated in to thermal, epithermal and fast region. The energy range of zero to 0.6 eV is related to thermal region, from 0.6 to 0.5 MeV is related to epithermal region and from 0.5 to 10 MeV is related to fast region too. The thermal region is the activation region for $^{nat}Cu(n,\gamma)^{64}Cu$ reaction so the thermal neutron distribution $\varphi(E)$ (n/(cm^2. s. MeV)) at the ^{nat}Cu target was calculated by F4/E4 card-MCNPX. The thermal flux in the target site was calculated about 4.5×10^{13} n.cm^{-2}.s^{-1} which is same as the experimental condition. The cross section $\sigma(E)$ (in barn) of $^{nat}Cu(n,\gamma)^{64}Cu$ reaction was calculated via TALYS-1.8 code in thermal neutron energy region and via these results, Eq. (3) was calculated about 2.042×10^{-10} n/s. At the end, the activity value was calculated by Eq. (1) about 38.32 GBq.

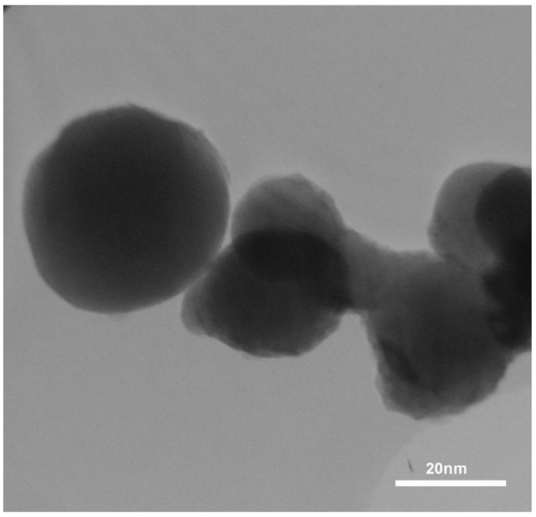

Fig. 5. TEM of copper nanoparticles from Iranian Nanomaterials Pioneers Company, NANOSANY.

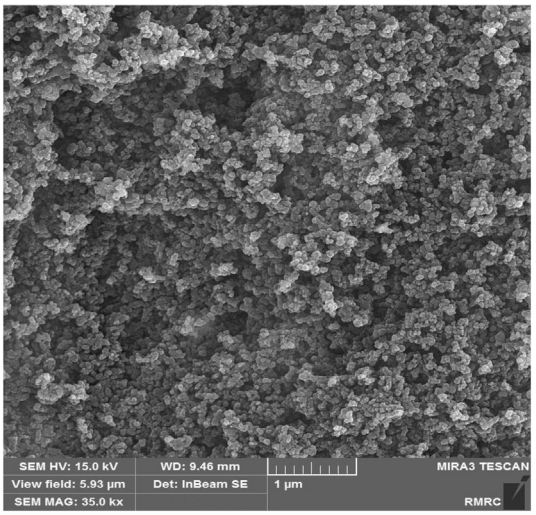

Fig. 6. SEM of copper nanoparticles from Iranian Nanomaterials Pioneers Company (NANOSANY), before irradiation process.

The saturated activity was calculated by FM4 card-MCNPX in three neutron energy regions as can be seen in Fig. 10. The maximum attainable activity was calculated in the thermal neutron energy region about 13.30×10^2 GBq. The activity value after 32 min irradiation time was calculated about 38.15 GB. The activity value of ^{64}Cu predicted by the MCNPX code was listed in Table 2.

3.4. Characterization of ^{nat}CuNPs

Figs. 5 and 6 show the TEM and SEM images and size distribution graph of ^{nat}CuNPs respectively. These figures show the size of 20 nm with spherical morphology. Fig. 7 shows the SEM images of ^{nat}CuNPs after irradiation in reactor core which shows no definite changes compared to nonradioactive samples so the size of 20 nm and spherical morphology of nanoscale copper were remained. Fig. 8 is related to XRD analysis of copper nanoparticles and also Fig. 9 is the XRD analysis after 6 months later when it was placed in the vicinity of the air. The storage condition of nanoscale powder was sealed in vacuum and was stored in cool and dry room and it should not be exposure to air because the damp reunion will affect its dispersion performance. XRD analysis clearly displayed the CuONPs chemical formula with 70 nm crystallite size in pick

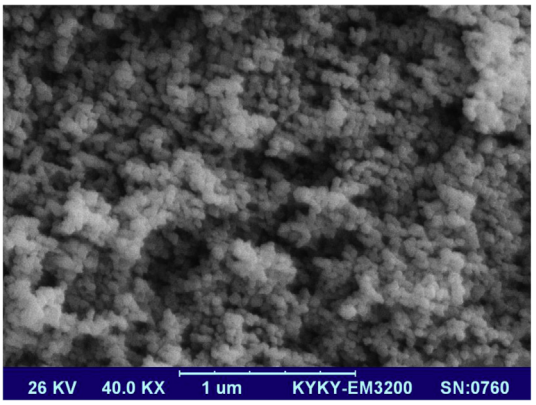

Fig. 7. SEM of copper nanoparticles from Digital Scanning Electron Microscope EM 3200 KYKY, after irradiation process.

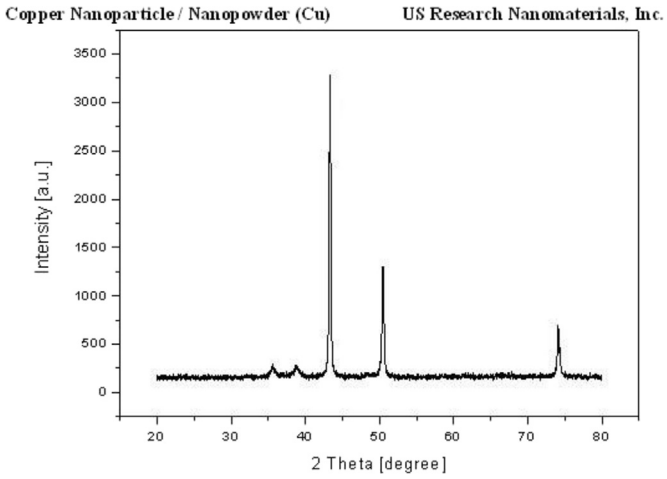

Fig. 8. XRD pattern of the copper nanoparticles from US Research Nanomaterials, Inc.

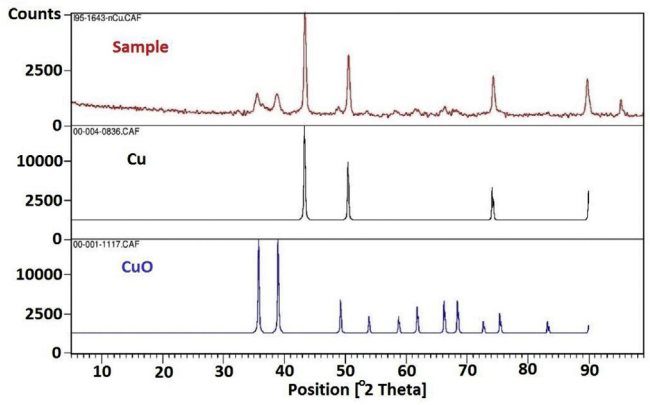

Fig. 9. XRD patterns of copper nanoparticles from STOE STADI, MP, Germany, after 6 months in the vicinity of the air.

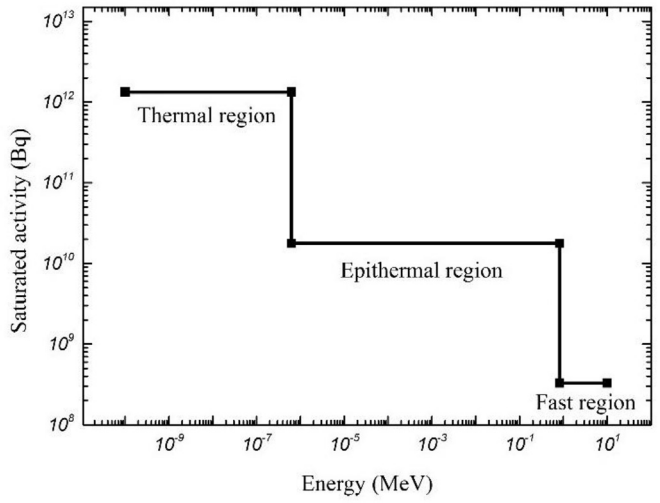

Fig. 10. Saturated activity of ^{64}Cu via ^{63}Cu(n,γ)^{64}Cu reaction in the different energy regions with FM4 card-MCNPX.

position of 35 were calculated by Eq. (2) and for CuNPs with 41 nm crystallite size in pick position of 43 with the scale factor of 6% and 94% for them respectively.

4. Conclusion

This study, was determined the production yields of ^{64}Cu via ^{63}Cu(n,γ)^{64}Cu reaction with ^{nat}Cu and ^{nat}CuNPs and showed increment activity of ^{64}Cu from ^{nat}CuNPs target. The cross sections values of this reaction were done with TALYS-1.8 code and had good adaptations with theoretical and available experimental cross section data. The activity of ^{64}Cu was calculated by using MCNPX code and theoretical methods. The good adaptations were achieved between the experimental results and calculated results, so the MCNPX can be used to optimize production condition in the reactor.

References

[1] A.H. Al Rayyes, Y. Ailouti, Production and quality control of ^{64}Cu from high current Ni target, World J. Nucl. Sci. Technol. 3 (2013) 72.
[2] http://www.nucleonica.net/wiki/index.php?title=Decay_Schemes.
[3] T.H. Bokhari, A. Mushtaq, I.U. Khan, Production of low and high specific activity ^{64}Cu in a reactor, J. Radioanal. Nucl. Chem. 284 (2010) 265–271.
[4] K.V. Vimalnath, A. Rajeswari, K.C. Jagadeesan, C. Viju, P.V. Joshi, M. Venkatesh, Studies on the production feasibility of ^{64}Cu by (n,p) reactions on Zn targets in Dhruva research reactor, J. Radioanal. Nucl. Chem. 294 (2012) 43–47.
[5] I.M. Cohen, M.S. Segovia, P.S. Bedregal, P.A. Mendoza, A.R. Aguirre, E.H. Montoya, A novel method for determination of copper in zinc destined to ^{64}Cu production in a nuclear reactor, J. Radioanal. Nucl. Chem. 309 (2016) 23–26.
[6] M. Neves, A. Kling, A. Oliveira, Radionuclides used for therapy and suggestion for new candidates, J. Radioanal. Nucl. Chem. 266 (2005) 377–384.
[7] A.M. Johnsen, B.J. Heidrich, C.B. Durrant, A.J. Bascom, K. Ünlü, Reactor production of ^{64}Cu and ^{67}Cu using enriched zinc target material, J. Radioanal. Nucl. Chem. 305 (2015) 61–71.
[8] M.R. Aboudzadeh, M.E. Moassesi, M. Amiri, H. Shams, B. Alirezapour, M. Sadeghi, et al., Preparation and characterization of chitosan-capped radioactive gold nanoparticles: neutron irradiation impact on structural properties, J. Iran. Chem. Soc. 13 (2015) 339–345.
[9] Z. Karimi, M. Sadeghi, N. Mataji-Kojouri, ^{64}Cu, a powerful positron emitter for immunoimaging and theranostic: production via ^{nat}ZnO and ^{nat}ZnO-NPs, Appl. Radiat. Isot. 137 (2018) 56–61.
[10] S.F. Hosseini, M. Sadeghi, M.R. Aboudzadeh, M. Mohseni, Production and modeling of radioactive gold nanoparticles in Tehran research reactor, Appl. Radiat. Isot. 118 (2016) 361–365.
[11] F. Soltani, A.B. Samani, M. Sadeghi, A.S. Shirvani, K. Yavari, Production of cerium-141 using ceria and nanoceria powder: a potential radioisotope for simultaneous therapeutic and diagnostic applications, J. Radioanal. Nucl. Chem. 303 (2015) 385–391.
[12] M.K. Bakht, M. Sadeghi, S.J. Ahmadi, S.S. Sadjadi, C. Tenreiro, Preparation of radioactive praseodymium oxide as a multifunctional agent in nuclear medicine: expanding the horizons of cancer therapy using nanosized neodymium oxide, Nucl. Med. Commun. 34 (2012) 5–12.
[13] IAEA, Vienna. Manual for reactor produced radioisotopes, IAEA-Tecdoc 1340 (2003) 63.
[14] M.B. Chadwick, M. Herman, P. Oblozinsky, M.E. Dunn, Y. Danon, A.C. Kahler, et al., ENDF/B-VII.1 Nuclear data for science and technology: cross sections, covariances, fission product yields and decay data, Nucl. Data Sheets 112 (2011) 2887–2996.
[15] A. Kara, M. Yiğit, T. Korkut, E. Tel, Cross section calculations of neutron induced reactions on ^{124,126,128,134,136}Xe, J. Fusion Energy 34 (2015) 882–886.
[16] M. Yiğit, Theoretical study of cross sections of proton-induced reactions on cobalt, Nucl. Eng. and Tech. 50 (2018) 411–415.
[17] M. Sadeghi, M. Enferadi, Nuclear model calculations on the production of ^{119}Sb via various nuclear reactions, Ann. Nucl. Energy 38 (4) (2011) 825–834.
[18] M. Yiğit, A. Kara, Simulation study of the proton-induced reaction cross sections for the production of ^{18}F and $^{66-68}$Ga radioisotopes, J. Radioanal. Nucl. Chem. 314 (2017) 2383–2392.
[19] S.F. Hosseini, M. Aboudzadeh, M. Sadeghi, A.A. Teymourlouy, M. Rostampour, Assessment and estimation of 67Cu production yield via deuteron induced reactions on ^{nat}Zn and ^{70}Zn, Appl. Radiat. Isot. 127 (2017) 137–141.
[20] M. Yiğit, Investigating the (p,n) excitation functions on $^{104-106,108,110}$ Pd isotopes, Appl. Radiat. Isot. 130 (2017) 109–114.
[21] M. Yiğit, Analysis of cross sections of (n,t) nuclear reaction using different empirical formulae and level density models, Appl. Radiat. Isot. 139 (2018) 151–158.
[22] A.J. Koning, S. Hilaire, S. Goriely, TALYS-1.8: a Nuclear Reaction Program. User Manual, NRG, Netherlands, 2013. http://www.talys.eu/download-talys.
[23] P. Saidi Bidokhti, M. Sadeghi, B. Fateh, M. Matloobi, G. Aslani, Nuclear data measurement of ^{186}Re production via various reactions, Nucl. Eng. and Tech. 42 (2010) 600–607.
[24] M. Yiğit, A. Kara, Model-based predictions for nuclear excitation functions of neutron-induced reactions on $^{64,\ 66-\ 68}$Zn targets, Nucl. Eng. and Tech. 49

(2017) 996–1005.
[25] M. Sadeghi, P. Sarabadani, H. Karami, Synthesis of maghemite nano-particles and its application as radionuclidic adsorbant to purify ^{109}Cd radionuclide, J. Radioanal. Nucl. Chem. 283 (2010) 297.
[26] M. Sadeghi, H. Karami, P. Sarabadani, F. Bolourinovin, Separation of the no-Carrier-added ^{109}Cd from Ag, Cu and ^{65}Zn by use of a precipitation and AG1-X8 resin, J. Radioanal. Nucl. Chem. 281 (3) (2009) 619–623.
[27] A. Hedayat, Simulation and transient analyses of a complete passive heat removal system in a downward cooling pool-type material testing reactor against a complete station blackout and long-term natural convection mode using the RELAP5/3.2 code, Nucl. Eng. and Tech. 49 (2017) 953–967.
[28] Z. Gholamzadeh, E. Bavarnegin, M.L. Rachti, S.M. Mirvakili, M.C. Dastjerdi, et al., Modeling of neutron diffractometry facility of tehran research reactor using VITESS 3.3a and MCNPX Codes, Nucl. Eng. and Tech 50 (2018) 151–158.
[29] M. Weigand, C. Beinrucker, A. Couture, S. Fiebiger, M. Fonseca, et al., Cu-63(n, γ) cross section measured via 25 keV activation and time of flight, Phys. Rev. C 95 (2017) 015808.
[30] E. Browne, J.K. Tuli, Nucl. Data Sheets 111 (2010) 1093.